Volume 52
Number 45
7 December 2023
Pages 16541-17044

Dalton Transactions

An international journal of inorganic chemistry

rsc.li/dalton

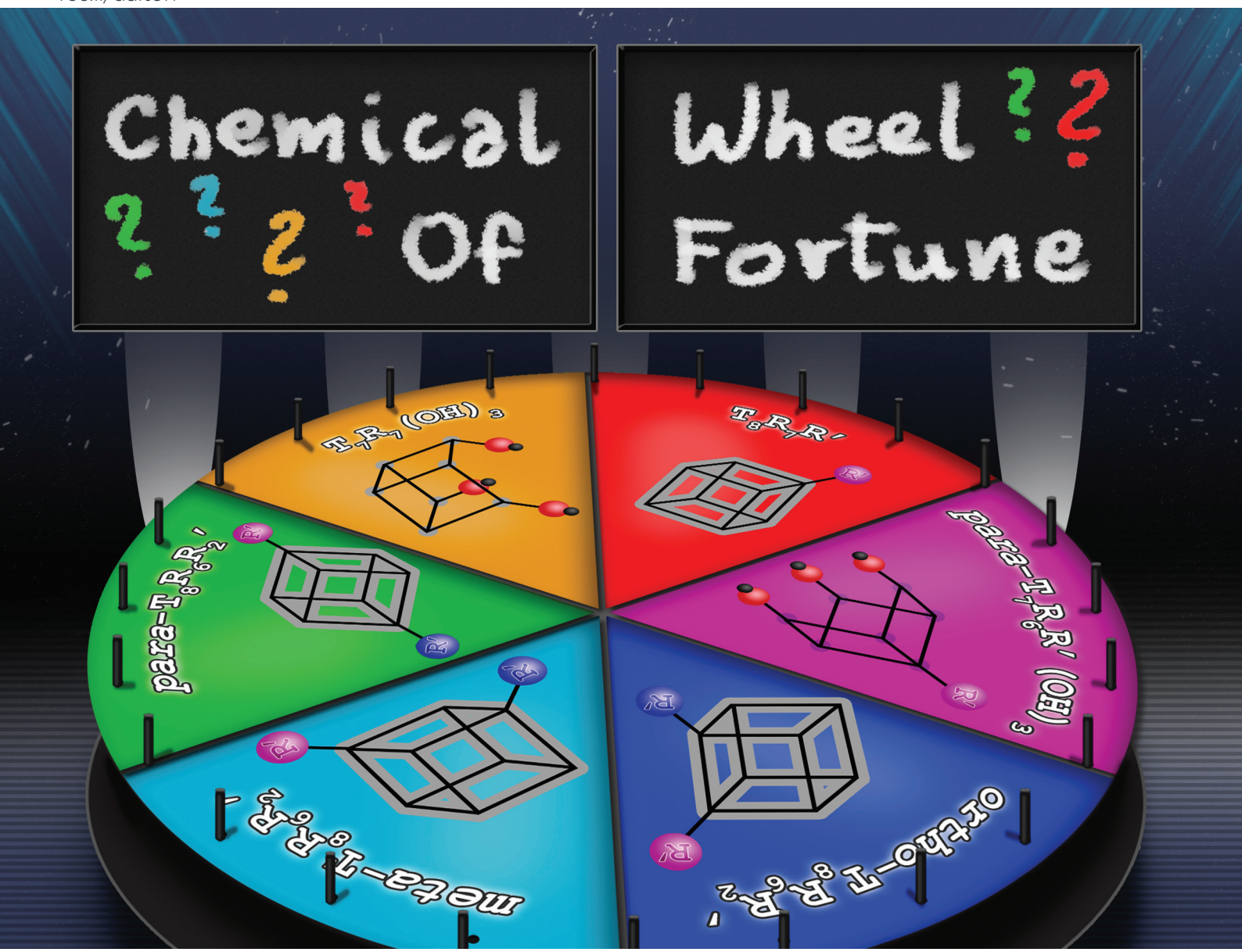

ISSN 1477-9226

ROYAL SOCIETY OF CHEMISTRY

PAPER

Łukasz John *et al.*

What do we know about bifunctional cage-like T_8 silsesquioxanes? Theory *versus* lab routine

Dalton Transactions

ROYAL SOCIETY OF CHEMISTRY

PAPER

View Article Online
View Journal | View Issue

Cite this: *Dalton Trans.*, 2023, **52**, 16607

What do we know about bifunctional cage-like T_8 silsesquioxanes? Theory *versus* lab routine†

Kamila Fuchs, [a] Edyta Nizioł, [a] Jolanta Ejfler, [a] Wiktor Zierkiewicz, [b] Anna Władyczyn [a] and Łukasz John *[a]

In this article, we explore theoretical validations of experimental findings pertaining to the classical corner-capping reactions of a commercially available heptaisobutyltrisilanol cage to mono-substituted phenylhepta (isobutyl)-POSS cages. Additionally, the process of opening a fully condensed cage is tracked to assess the possibility of isolating and separating the resulting isomers. The corner-capping reactions of potential silanotriols, both as monomers and dimers, and the impact of these structural motifs on their closing to bifunctional POSS cages are also investigated. Our studies highlight that analyzing experimental results alone, without incorporating complex theoretical investigations, does not offer a clear understanding of the reactions involving multiple simultaneously reacting substrates, which may also undergo further transformations, potentially complicating the conventional pathways of classic corner-opening/capping reactions.

Received 13th August 2023,
Accepted 27th September 2023

DOI: 10.1039/d3dt02638h

rsc.li/dalton

Introduction

Octafunctional polyhedral oligomeric silsesquioxanes (POSSs) of general formula $(RSiO_{3/2})_8$ (namely T_8R_8; T_8 is an octahedral cage containing eight silicon atoms; R is the reactive or non-reactive group or hydrogen atom) constitute an attractive group of organosilicons with hybrid architecture.

In the case of cubic derivatives, the silsesquioxane core comprises eight silicon atoms connected *via* oxygen bridges. The siloxane moieties forming an inorganic core impart tremendous thermodynamic, mechanical, and chemical stability. Moreover, various organic groups can modify the vertices of the inner cube. Among the T_8-type silsesquioxanes, the most recognized are mono- (Fig. 1A) and octafunctional (Fig. 1B) derivatives routinely obtained from, *e.g.*, octakis(3-aminopropyl)octasilsesquioxane or octakis(vinyl)octasilsesquioxanes.[1] The third type of cage-like silsesquioxanes, which have not been widely studied, can be considered a surrogate to *cis*/*trans* bifunctional double-decker silsesquioxanes (DDSQs).[2] Bifunctional derivatives of silsesquioxanes shown in Fig. 1C are predominantly synthesized using corner-opening and corner-capping strategies.[3] Unusually, there are only a small number of literature reports on this topic, considering the potential of bifunctional POSSs as precise nano-building blocks for advanced materials (*e.g.*, polymers, dendrimers, and Janus silsesquioxanes) with peculiar properties in a bottom-up approach.[4] On the other hand, accurately positioning functional groups in custom-designed architectures through precise synthesis can be an overwhelming challenge.[5–13]

So far, little reliable evidence has been presented for obtaining POSSs with several (less than 8 in the case of octa-substituted derivatives) reactive substituents.[14] There is also a lack of information on this type of organosilicon compounds' crystal structures. The only shreds of evidence of obtaining

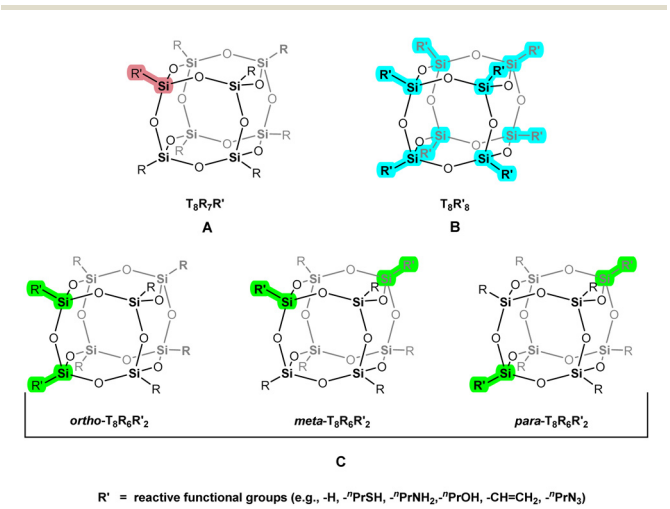

Fig. 1 Possible cubic T_8-type silsesquioxanes: (A) monofunctional, (B) octafunctional, and (C) bifunctional.

[a]*Faculty of Chemistry, University of Wrocław, 14 F. Joliot-Curie, 50-383 Wrocław, Poland. E-mail: lukasz.john@uwr.edu.pl*
[b]*Faculty of Chemistry, Wrocław University of Science and Technology, 27 Wybrzeże Wyspiańskiego, 50-370 Wrocław, Poland*

†Electronic supplementary information (ESI) available: ^1H, ^{13}C, ^{29}Si spectra, FT-IR spectra, MALDI-MS spectra, quantum calculations data. See DOI: https://doi.org/10.1039/d3dt02638h

such structures are low-quality ^{29}Si NMR spectra.[15,16] Conclusions drawn from interpreting the number and position of signals in the ^{29}Si NMR spectrum are insufficient to formulate a definite assumption on the structure of caged silsesquioxane, as other analytical methods should support such findings. W.-B. Zhang[14] presented the evidence of bifunctional (and also trifunctional) POSS describing the preparation of heterofunctional POSSs by modification of an octa-vinyl-substituted silsesquioxane cage. As a result, some of the vinyl groups are modified under the influence of trifluoroacetic acid to hydroxyethyl groups. The use of a 5-fold excess of acid and a short reaction time (4–5 h) caused the vinyl substituents to react partially – thus, a mixture of POSS substituted with vinyl and hydroxyethyl groups in different proportions and positions was obtained. A relatively short reaction time was necessary in this case because it was observed that the extension of the reaction time destroys the cage structure due to the hydrolysis of Si–O and Si–C bonds. As a result of 'multi-variant' column chromatography, it was possible to separate the *para* (D_{3d}, 4% yield), *ortho* (C_{2v}, 10%), and *meta* (C_{2v}, 10%) isomers in a ratio of 1/3/3 and three isomers for the trifunctional cage, which was confirmed by NMR spectroscopy (^{29}Si, ^{1}H, and ^{13}C). In addition, the results described by B. Dudziec, P. Żak, *et al.*[17] on cross-metathesis, where octa-vinyl-substituted POSS was also used as a substrate for further modifications, confirm that such reactions occur non-stoichiometrically, obtaining a mixture of products with varying degrees of substitution.

The selective synthesis of derivatives with more than one reactive substituent is problematic because the hydrolytic condensation of trihalo/trialkoxy silanes is a complicated equilibrium process. The selectivity of the reaction is influenced not only by the stoichiometry of the reactants but also by the type of solvent, temperature, or catalyst.[18] The products of hydrolytic condensation using a mixture of trichloro/trialkoxy silanes differing in substituent have been proven to be a mixture of octa-T_8R_8, mono-T_8R_7R', bifunctional $T_8R_6R'_2$ (*para*, *ortho* and *meta* isomers) cages, and polysilsesquioxanes.[16,19] Among the inconveniences associated with obtaining pure, hetero-functional T_8 cages, one can also mention the problem with their separation.[20] These derivatives have a similar structure (and thus polarity) and tend to form weak intermolecular interactions. These factors are the basis for the coelution of the components of the mixture of heterosubstituted derivatives and geometric isomers of bifunctional cages. Therefore, POSS derivatives are sought, the synthesis of which would be scalable, reproducible, and relatively inexpensive.

L. Marchese *et al.*[21] developed a method for the synthesis of bifunctional POSSs, in which the monofunctional POSS was used as a starting material, which undergoes hydrolysis in only one corner of the cage (so-called corner-opening reaction). The hydrolysis was carried out in THF in the presence of tetramethylammonium hydroxide (TEAOH) for 4 h under reflux. Next, the opened cage reacts with $Ti(O^iPr)_4$, forming a new cage through condensation. The resulting cage possesses six isobutyl groups, one 3-aminopropyl group, and a titanium atom embedded in the cage structure with a coordinated isopropoxy group located in the *para* position relative to it. The chance of success of this strategy comes from the assumption that the hydrolysis of the monofunctional cage is favored for one of the corners of the cage. According to this report, the Si atom in the *para* position to the 3-aminopropyl substituent and the Si atom with the 3-aminopropyl substituent undergo hydrolysis, with the efficiency of the first process being as much as 88% and 12% for the second one. The main product of the synthesis was probably identified based on the number of signals in the ^{29}Si NMR spectrum. *para*-Adduct is the most symmetrical isomer; it has three Si atoms with the same chemical environment, so the number of signals for this isomer is 3; for *ortho*-adduct and *meta*-adduct, five signals are expected. Unfortunately, the authors do not explain how the $T_7R_7(OH)_3$ open cage was separated from the $T_7R_6R'(OH)_3$ cage. It is also not entirely clear which premise the percentage content of the mixture products was determined. The mentioned concept inspired K. Naka[15,21] to apply this strategy to introduce the same silane into the hydrolyzed corner used at the monofunctional cage synthesis stage. First, the authors repeated the procedure by opening the 3-aminopropyl heptaisobutyl cage in the presence of TEAOH. Next, the hydrolysis product was purified by washing with methanol, which probably caused the isolation of $T_7R_7(OH)_3$ from the reaction mixture. The authors extended the reaction time from 4 to 7 h, obtaining the $T_7R_6R'(OH)_3$ derivative with a 93% yield. The next step involved the open cage reaction with the 3-aminopropyl substituent with 3-aminopropyltriethoxysilane.[22] The reaction was carried out in THF at room temperature for 48 h. The bifunctional cage was obtained after dissolving the reaction mixture in methanol, concentrating the filtrate, and washing it with acetonitrile, with a good yield of 68%. The fact that the *para* isomer was obtained is supported by the ^{29}Si NMR spectrum with two signals (which is the expected effect for a symmetric *para* isomer). However, the resolution of the published spectrum is poor, and the signal integration ratio does not agree with the theoretical one. For the *para* isomer, two signals with 2 : 6 integration are expected, whereas this report equals 1 : 1. This work is also enriched with DFT calculations, the result of which explains the preference of nucleophilic attack for the silicon atom in the *para* position.

A similar synthetic strategy was used to prepare bivinylheptaisobutyl-POSS.[15] Vinylheptaisobutyl-POSS was used as a precursor for the corner-opening reaction. The reaction was carried out at room temperature and not, as in the case of 3-aminopropylheptaisobutyl-POSS, noticing fewer chemical shifts in the spectrum. The analysis of multinuclear (^{29}Si, ^{1}H, and ^{13}C) NMR and FT-IR spectra proves that carrying out the reaction at a lower temperature leads to the selective formation of an open cage in the *para* position. After the reaction, an appropriate amount of 2 M HCl solution was introduced to separate the product of its reaction with TEAOH from the post-reaction mixture. The mixture was then concentrated, methanol was added to the residue, and the formed precipitate (probably unreacted substrate) was filtered off. The product was obtained as a precipitate after the concentration of the

solution and drying in a vacuum. Then, the dried product was used in the corner-capping procedure. As a second substrate, trichlorovinyl silane was used, which was applied in a slight excess relative to POSS. The reaction was carried out for 1 h at 0 °C and then for 3 h at room temperature.

Interestingly, the authors did not use the addition of a tertiary amine (such as TEA or DIPEA) in this reaction, which is typically used in corner-capping reactions to neutralize HCl released as a byproduct. Adding an amine increases the yield of the reaction for two reasons. Firstly, it shifts the reaction equilibrium towards product formation. Secondly, it neutralizes HCl, which can cause cage hydrolysis. The reaction mixture was concentrated, and the pure product was purified by size exclusion chromatography, leading to bi(vinyl)hexaisobutyl-POSS. It is worth mentioning that the postulated efficiency of obtaining a bifunctional cage after purification by this method is only 20%. The purification method by fractional crystallization using propane-2-ol and acetonitrile reported a yield of 50%; however, further optimization of the synthesis and purification is needed.

In this paper, the quest for *ortho*, *meta*, and *para* isomers, as a part of the enigmatic synthesis of bifunctional $T_8R_6R'_2$ POSS, from theoretical and experimental standpoints, is deeply analyzed and discussed.

Experimental section

Materials and methods

All commercially available chemicals were used without further purification: phenyltrimethoxysilane (>97%, Sigma Aldrich), isobutyltrisilanol POSS (Hybrid Plastics Inc.), tetraethyl–ammonium hydroxide (35% w/w aq. soln., Alfa Aesar), hydrochloric acid solution (2 M, Sigma Aldrich). Solvents for standard workup (tetrahydrofuran, ethanol, methanol, acetonitrile) were used as received and were purchased from Chempur and VWR International. Elemental analyses were measured on an Elementar's Vario EL Cube analyzer. The NMR spectra were recorded with the Bruker Avance II 500 MHz spectrometer and Bruker Avance III 600 MHz spectrometer. The solvent used during the measurements was chloroform. Spectra were calibrated based on the residual solvent signal, taking the following values: 7.26 ppm for ^{1}H NMR spectra and 77.00 ppm for ^{13}C NMR spectra. FTIR spectra were recorded on Bruker Vertex 70 spectrometer. The measured samples were prepared by making a KBr pellet. MALDI-MS spectra were recorded using JEOL JMS-S3000 SpiralTOF™-plus Ultra-High Mass Resolution MALDI-TOFMS Mass Spectrometer.

Synthetic procedures

Synthesis of phenylhepta(isobutyl)-POSS T_8(i-Bu)$_7$(Ph) (1). 1 was synthesized following the method reported by Blanco *et al.*[23] Isobutyltrisilanol (3.95 g, 5.0 mmol) was dissolved in 50 mL of ethanol and phenyltrimethoxysilane (1.03 g, 5.2 mmol), and 2.0 mL of tetramethylammonium hydroxide (TEAOH) was added under stirring. The clear solution was stirred at room temperature for 24 h. The resulting solid was filtered and washed with two portions (10 mL) of anhydrous ethanol and then dried under reduced pressure to give the desired compound with 85% yield. Elemental analysis (%) for $C_{34}H_{68}O_{12}Si_8$: calcd, C 45.70, H 7.67, Si 25.14; found, C 45.58, H 7.73, Si 25.07. ^{1}H NMR (500 MHz, $CDCl_3$), δ (ppm): 7.66–7.61 (m, 2H), 7.43–7.37 (m, 1H), 7.36–7.31 (m, 2H), 1.95–1.73 (m, 7H), 1.00–0.86 (m, 42H), 0.65–0.56 (t, 14H). ^{13}C NMR (126 MHz, $CDCl_3$), δ (ppm): 134.01 (s, 2C), 131.84 (s, 1C), 130.24 (s, 1C), 127.59 (s, 2C), 25.68 (d, 14C) 23.87 (s, 7C), 22.54 (s, 7C). ^{29}Si NMR (500 MHz, $CDCl_3$), δ (ppm): 68.35, 67.57, 67.37, 58.22. FT-IR (cm^{-1}, KBr): ν_{CH} 2955 (m), ν_{CH} 1466 (s), δ_{CH3} 1367 (s) ν_{Si-CH} 1231 (s), $\nu_{Si-O-Si}$ 1114 (s), δ_{CH} 838 (s), δ_{CH} 746 (m), δ_{O-Si-C} 486 (s). MALDI-MS *m*/*z*: 915.27 {calcd for $[M + Na]^+$ 915.28}.

Synthesis of trisilanols phenylhexa(isobutyl)-POSS; *ortho*/*meta*/*para*-T_7(i-Bu)$_6$(Ph)(OH)$_3$ (2). To a solution of **1** (1.00 g, 1.12 mmol) in THF (20 mL), an equimolar amount of 35% aqueous TEAOH solution (0.16 mL, 1.12 mmol) was added, and the mixture was stirred under reflux (80 °C) for 7 h. Next, the reaction mixture was neutralized with 2 M aqueous HCl. The salts were removed by filtration, and volatiles and THF were evaporated on the rotary evaporator. The residue was dispersed in methanol and dried under vacuum. The resulting trisilanol **2** was obtained with a 76% yield. Elemental analysis (%) for $C_{30}H_{62}O_{12}Si_7$: calcd C 44.41, H 7.70, Si 24.23; found, C 44.36, H 7.72, Si 24.23. ^{1}H NMR (600 MHz, $CDCl_3$), δ (ppm): 7.63–7.61 (m, 2H), 7.42–7.37 (t, 1H), 7.34–7.32 (d, 2H), 1.85–1.81 (m, 6H), 0.94–0.93 (dd, 36H), 0.60–0.56 (m, 12H). ^{13}C NMR (126 MHz, $CDCl_3$), δ (ppm): 134.02 (s, 2C), 133.93 (s, 1C), 130.20 (s, 1C), 127.61 (s, 2C), 25.77–25.73 (d, 12C), 23.93–23.90 (d, 6C), 23.10 (s, 3C), 22.80 (s, 3C). ^{29}Si NMR (99 MHz, $CDCl_3$), δ (ppm) 58.46, 67.41, 68.49. FT-IR (cm^{-1}, KBr): ν_{OH} 3271(s), ν_{CH} 2954 (s), ν_{CH} 1466 (m), δ_{CH3} 1366 (m) ν_{Si-CH} 1229 (s), $\nu_{Si-O-Si}$ 1124 (s), δ_{CH} 837 (m), δ_{CH} 741 (m), δ_{O-Si-C} 481 (m). MALDI-MS *m*/*z*: 833.25 {calcd for $[M + Na]^+$ 833.25}.

Diphenylhexa(isobutyl)-POSS T_8(i-Bu)$_6$(Ph)$_2$ synthesis attempt

0.5 g of **2** (0.6 mmol) was dissolved in 20 mL of THF, and phenyltrimethoxysilane (0.122 g, 0.6 mmol) was added when stirring. The solution was stirred at room temperature for 48 h, and then THF was evaporated on the rotary evaporator. The residue was dispersed in 30 mL of acetonitrile and dried under vacuum. The identified reaction product was partially condensed trisilanol T_7(i-Bu)$_7$(OH)$_3$ (**3**) instead of T_8(i-Bu)$_6$(Ph)$_2$, which was obtained with 83% yield. ^{1}H NMR (500 MHz, $CDCl_3$), δ (ppm): 6.80 (s, 3H), 1.84 (m, 7H), 0.93 (dd, 42H), 0.55 (m, 14H). ^{13}C NMR (126 MHz, $CDCl_3$), δ (ppm): 25.78 (d, 14C) 23.91 (s, 7C), 23.27 (s, 4C), 22.86 (s, 3C). ^{29}Si NMR (99 MHz, $CDCl_3$), δ (ppm): 59.00, 67.48, 68.74. MALDI-MS *m*/*z*: 813.26 {calcd for $[M + Na]^+$ 813.28}.

Theoretical calculations

Optimizations and molecular orbitals for all structures presented in this article were calculated at the B3LYP-D3/6-31g(d) (hybrid density functional with D3 damping function to

include dispersion) level of theory in the gas phase.[24–27] The optimizations were conducted without any geometrical constraints, and the vibrational frequencies were calculated to confirm that all obtained geometries are true minima, as there were no imaginary frequencies. All optimizations were carried out in Gaussian16, Rev.C.O1 set of codes.[28] The Chemcraft[29] software was applied to visualize molecular orbitals.

Theoretical diffusion coefficients (D) have been calculated for DFT optimized structures following the Einstein–Stokes equation, corrected by a factor derived from micro-frictional theory[30] and semi-empirically improved by Chen[31] eqn (1), where k is Boltzmann constant, T is the temperature, and η is the viscosity of deuterated benzene.[32] Spherical equivalent radii ($R_{eq.}$) have been calculated from volumes limited by the van der Waals surface (V) eqn (2). van der Waals volumes have been calculated using MultiWFN software[33,34] and visualized in the VMD program.[35]

$$D = \left(\frac{kT}{6\pi\eta R_{eq}}\right)\left(1 + 0.695\left(\frac{R_s}{R_{eq}}\right)^{2.234}\right) \quad (1)$$

$$R_{eq} = \sqrt[3]{\frac{3V}{4\pi}} \quad (2)$$

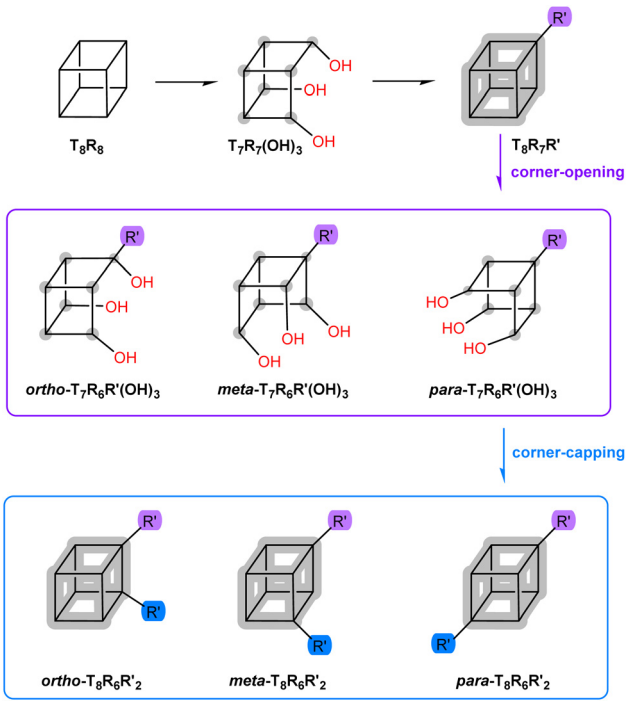

Fig. 2 Transformation of octa-substituted T_8R_8 to bifunctional $T_8R_6R'_2$ cages.

Results and discussion

The strategic synthesis of bifunctional POSS cages ($T_8R_6R'_2$) is highly significant in developing novel hybrid compounds with exceptional properties. Achieving selectivity in the placement of sidearms at the *ortho* (*o*), *meta* (*m*), or *para* (*p*) positions is crucial. The traditional approach involves opening the T_8 octafunctional (T_8R_8) cage, followed by closing the resulting $T_7R_7(OH)_3$ silanotriol to form the monofunctional POSS (T_8R_7R') cage. The closing step is typically uncomplicated, and the reaction efficiency and product yield depend on the characteristics of the substituents on the cage core and the optimization of the corner-capping reaction. However, reopening the cage lacks selectivity, resulting in a mixture of *ortho*/*meta*/*para* silanotriols of formula $T_7R_6R'(OH)_3$ (Fig. 2). The separation of this mixture or the selective closure of a monofunctional derivative holds great significance for the synthesis of bifunctional $T_8R_6R'_2$ cages.

Finding a solution to this problem remains one of the most intriguing synthetic strategies in silsesquioxane cage chemistry. Consequently, a controlled process necessitates selective reactions involving the closing and opening of monofunctional T_8R_7R' cages (Fig. 2).

The initial step in the 'transformation' process involves opening the octafunctional T_8R_8 cage, which is straightforward, and the resulting product, the silanotriol $T_7R_7(OH)_3$, is readily available commercially. Similarly, closing a silanotriol to form a mono-POSS cage (T_8R_7R') is not problematic as long as there is no condensation reaction between the hydroxyl groups of the open cages. Such condensation could lead to contamination with the T_8R_8 cage or several other difficult-to-identify byproducts. Another factor that disrupts corner-capping reactions is the formation of the $[T_7R_7(OH)_3]_2$ dimer through intermolecular hydrogen bonds among the $T_7R_7(OH)_3$ silanotriols. The contamination of the main product with the T_8R_8 cage can be detected using ^{29}Si NMR spectroscopy or mass spectrometry. However, identifying the $[T_7R_7(OH)_3]_2$ dimer and controlling its reactivity is neither straightforward nor trivial. Similar challenges arise with monofunctional open cages, namely *o*/*m*/*p* $T_7R_6R'(OH)_3$, where the statistical opening of the T_8R_7R' cage increases the number of potential combinations, including the possibility of dimer formation. In this case, none of the T_8R_7R' silicon atoms is favored in the hydrolysis reaction, resulting in a mixture of monomeric regioisomers *o*/*m*/*p*-$T_7R_6R'(OH)_3$, as well as homo(*o*–*o*, *p*–*p*, *m*–*m*) and hetero(*o*–*p*, *o*–*m*, *p*–*m*) combinations. Unusual rearrangements of cages or unintended closures can be confirmed when these compounds crystallize, providing an opportunity to assess the potential synthesis strategy.

This study focuses on the hindrance of further cage corner-capping reactions caused by the crystallization of a stable dimer. Consequently, computational methods were employed to analyze this issue and determine the crucial factors in evaluating the reactivity of POSS mono-cages in both closed T_8R_7R', $T_8R_6R_2'$, and open states. The open cages, specifically silanotriols, exist as monomers and dimers denoted as $T_7R_6R'(OH)_3$ and $[T_7R_6R'(OH)_3]_2$, respectively. In these structures, R represents i-Bu or Ph, while R′ represents 3-aminopropyl ($C_3H_6NH_2$), vinyl (C_2H_3), or phenyl (Ph). The closed derivatives ($T_8R_6R'_2$) exhibit *ortho*, *meta*, and *para* isomers. Similarly, open

forms, both as monomeric and dimeric silanotriols, are mixtures of *o*/*m*/*p* isomers (Fig. 3).

In order to gain insight into the reactivity of closed POSS forms in corner-capping reactions and open forms in corner-opening reactions, DFT calculations were performed. The optimized structures of closed POSS cages were analyzed to examine the patterns of the Lowest Unoccupied Molecular Orbital (LUMO) and its neighboring unoccupied MOs, which play a role in nucleophilic attacks initiating corner-opening reactions. The LUMO pattern was also calculated for open forms and bifunctional POSS cages (Table S1 and Fig. S19†).

The starting point for optimization of dimer structures was based on the known crystal structures of the silanotriol dimers $[T_7(i\text{-}Bu)_7(OH)_3]_2$, which crystallize in the monoclinic crystallographic system in the space group $P2_1/n$.[36–39] Two open cage molecules are connected by three hydrogen bonds between the silanol groups (the distances between adjacent oxygen atoms of the hydroxyl groups are between 2.64–2.68 Å); molecules creating dimer are symmetry-related by inversion center (Fig. S16†). The dimer reported by F. Feher *et al.*[39] was observed to crystallize during the condensation reaction of cyclohexyltrichlorosilane in aqueous acetone, with the crystallization process lasting from several months to 3 years (!). The dimer crystallized in the mixture containing T_8R_8 (R = i-Bu) cages and an unusually open $T_8R_8(OH)_2$. On the other hand, a dimer with phenyl substituents could be obtained within a few minutes by reacting the $T_7R_7(ONa)_3$ derivative with an aqueous HCl solution, as reported by Liu *et al.*[37] The same group also described the equilibrium between these cages and another dimer structure.[40] In each case, confirming the structure of the main dimer product required a lengthy crystallization period. Additionally, the products of unusual transformations crystallized only after isolating the dimer, and it was through long-term crystallization and determination of the crystal structure that these structural motifs could be diagnosed. X-ray data confirmed the synthesis of cages with unique structures, but they did not offer clear guidelines for planning effective synthesis strategies or proposing reaction equations with absolute certainty.

The structure in the solid state may or may not be consistent with that in the solution after the crystals have dissolved. In the most straightforward approach, dimer, monomer, or monomer-dimer dynamics may be in solution. In order to verify whether the dimer motif is maintained in solution, the experimental diffusion coefficient (D_{exp}) determined from the DOSY spectra and the theoretical one were compared using the methodology presented in our previous work.[41] The diffusion coefficient (D) for trisilanol (**3**) from the experimental studies is close to that calculated for the monomer (Fig. 4 and Table 1). Similarly, for silanols (**2**), the D_{exp} is consistent with D_{DFT} for monomeric form. The careful analysis of experimental data and their validation through computational methods suggest that the dimeric motif is prevalent in the crystalline form. At the same time, monomers are the dominant species in solution.

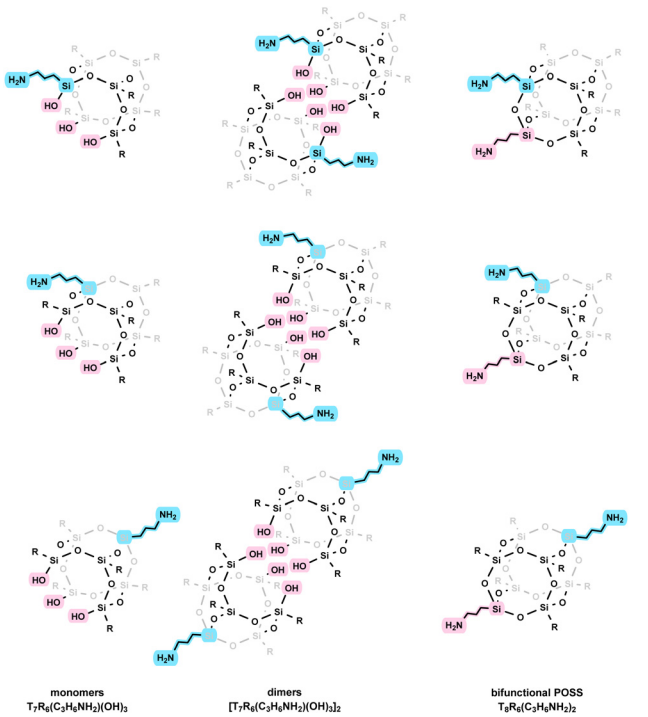

Fig. 3 Examples of monomers and dimers in opened versions as *ortho*, *meta*, and *para* isomers: $T_7R_6(C_3H_6NH_2)(OH)_3$, and $[T_7R_6(C_3H_6NH_2(OH)_3)]_2$, and closed bifunctional $T_8R_6(C_3H_6NH_2)_2$ cages.

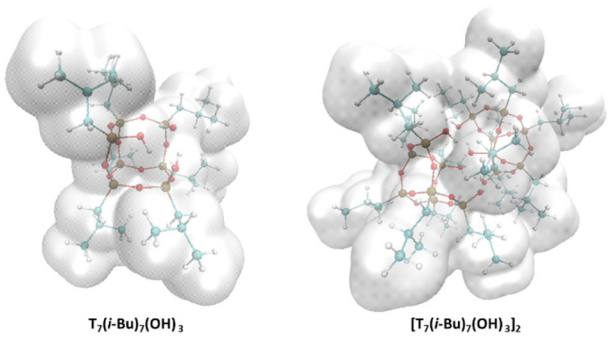

Fig. 4 van der Waals surfaces generated around DFT optimized $T_7(i\text{-}Bu)_7(OH)_3$ and $[T_7(i\text{-}Bu)_7(OH)_3]_2$ structures.

Table 1 van der Waals volumes (V), theoretical diffusion coefficients (D_{DFT}), and experimental diffusion coefficient (D_{exp}) for DFT optimized structures of POSS cages

POSS	V [Å]	D_{DFT} [$m^2\ s^{-1}$]	D_{exp} [$m^2\ s^{-1}$]
$T_7(i\text{-}Bu)_7(OH)_3$	979.800	6.7×10^{-10}	6.1×10^{-10}
$[T_7(i\text{-}Bu)_7(OH)_3]_2$	1945.593	5.1×10^{-10}	—
ortho-$T_7(i\text{-}Bu)_6(Ph)(OH)_3$	982.897	6.7×10^{-10}	6.8×10^{-10}
[*ortho*-$T_7(i\text{-}Bu)_6(Ph)(OH)_3]_2$	1955.177	5.1×10^{-10}	—
meta-$T_7(i\text{-}Bu)_6(Ph)(OH)_3$	982.688	6.7×10^{-10}	6.8×10^{-10}
[*meta*-$T_7(i\text{-}Bu)_6(Ph)(OH)_3]_2$	1955.478	5.1×10^{-10}	—
para-$T_7(i\text{-}Bu)_6(Ph)(OH)_3$	983.848	6.7×10^{-10}	6.8×10^{-10}
[*para*-$T_7(i\text{-}Bu)_6(Ph)(OH)_3]_2$	1947.774	5.1×10^{-10}	—

To gain a deeper understanding of the factors influencing the transition of silanotriol structures from monomers to dimers, theoretical investigations were conducted on T_8R_8 cage structures featuring phenolic and isopropyl substituents. The computational results for open cages, both monomers and dimers, with i-Bu substituents and closed bifunctionalized cages possessing 3-aminopropyl sidearms are presented in Fig. 5. Additionally, Fig. S18 and Table S2† exhibit other results for cages of this type but containing vinyl and phenyl arms.

Theoretical and experimental studies confirm that, in each instance, dimers exhibit greater stability. This is evident from the crystallization of open cages in their dimeric form from concentrated solutions. However, when the solutions are more dilute, dissociation occurs, leading to the dominance of open cages in the form of monomers. There are notable distinctions

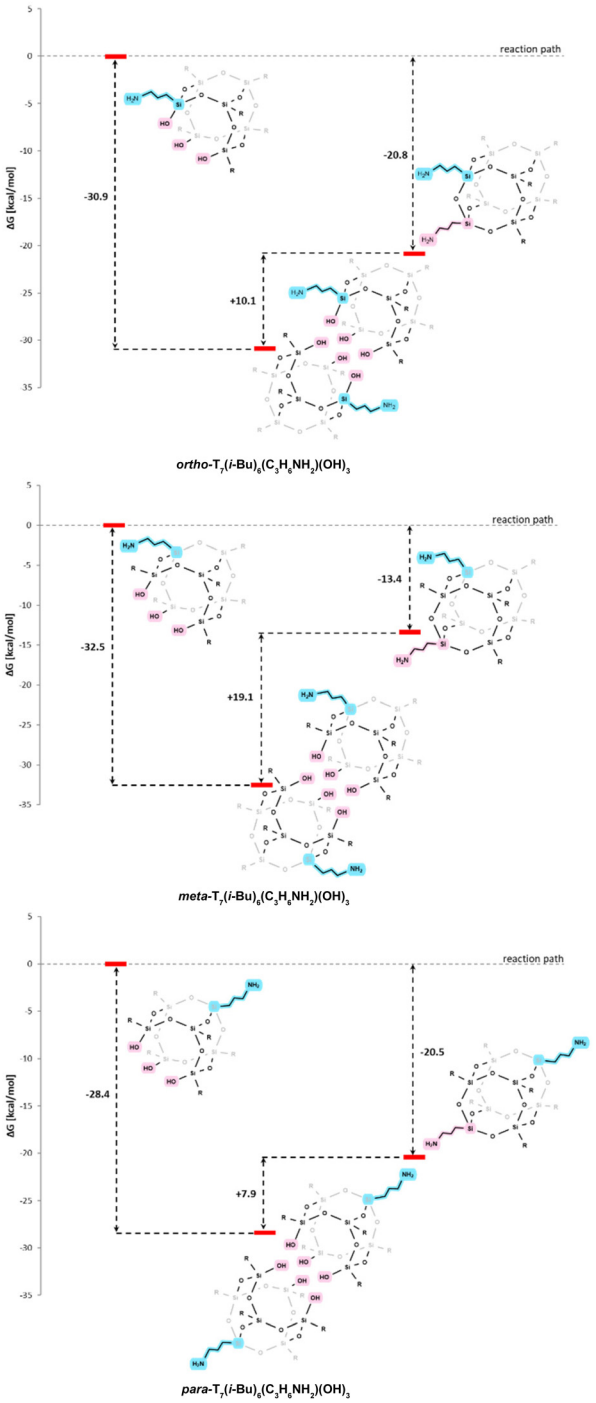

Fig. 5 Relative Gibbs free energies (kcal mol^{-1}) for DFT optimized POSS structures with a 3-aminopropyl sidearm.

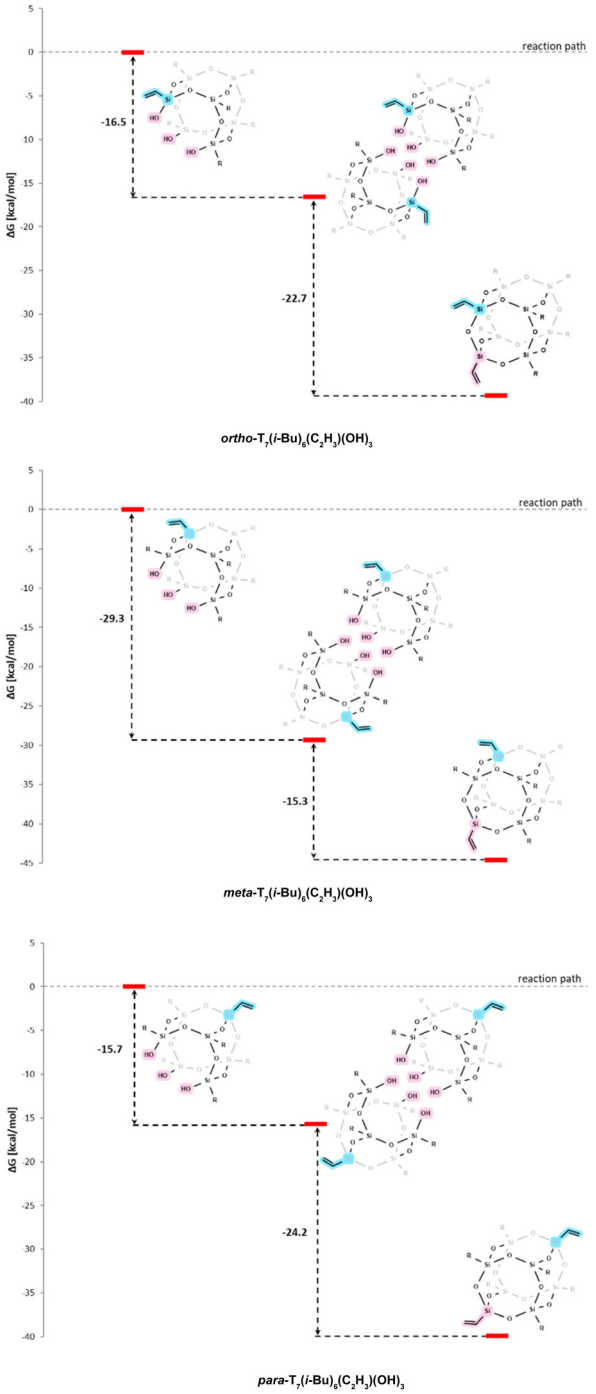

Fig. 6 Relative Gibbs free energies (kcal mol^{-1}) for DFT optimized POSS structures with a vinyl arm.

between cages with 3-aminopropyl and vinyl sidearms. Regarding cages with a core featuring i-Bu and Ph substituents and a 3-aminopropyl substituent, dimers exhibit lower reactivity than monomers (Fig. 5, Fig. S18†). Corner-capping reactions for dimers require higher energies, with the *meta* form being the least reactive.

A contrasting scenario arises for cages with a vinyl arm, as depicted in Fig. 6 and Fig. S18.† In these cases, both monomers and dimers undergo spontaneous corner-capping reactions. Similarly, the *meta* form is less reactive. However, these differences are not substantial enough to significantly impact the regioselectivity of the reaction.

Subsequent HOMO/LUMO investigations reveal the possibility of distinguishing the reactivity of individual forms (Fig. 7, Fig. S19 and Table S1†). Among cages featuring an i-Bu substituent in the core, the most negligible energy difference is observed for mono-POSS with a phenyl arm. This suggests its heightened susceptibility to corner-opening reactions; however, the differences are insignificant compared to cages with a vinyl or 3-aminopropyl sidearm. The open forms of silanotriols exhibit comparable reactivity, with a slight decrease in activity observed for the *meta* form (Fig. 8).

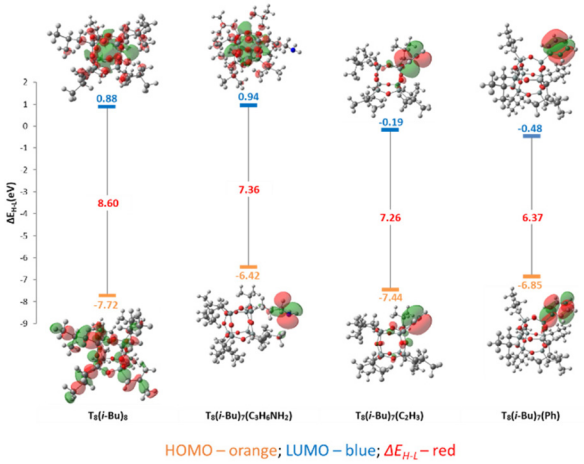

Fig. 7 Calculated HOMO (orange) and LUMO (blue) energy levels and their visualization, and HOMO–LUMO energy gaps (red) of optimized mono-POSS models with different arms: i-Bu, vinyl, amine, phenyl.

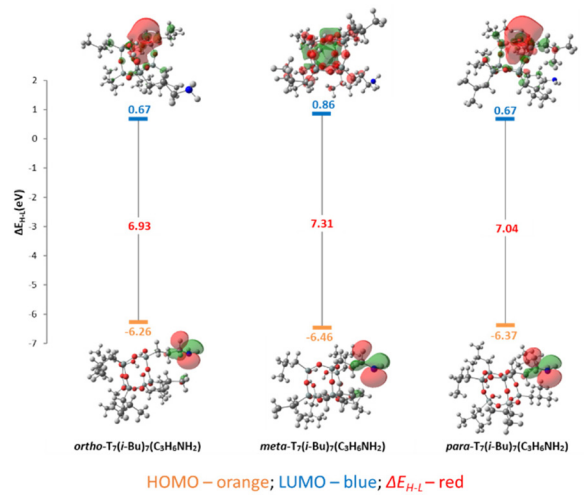

Fig. 8 Calculated HOMO (orange) and LUMO (blue) energy levels and their visualization, and HOMO–LUMO energy gaps (red) of optimized open-POSS models with amine arms.

Conclusions

In conclusion, the strategic synthesis of bifunctional POSS cages ($T_8R_6R'_2$) seems significant for developing novel hybrid compounds with exceptional properties. However, achieving selectivity in placing sidearms at different positions (*ortho*, *meta*, and *para*) is demanding, if at all possible, with reasonable yield. The traditional approach involves opening the T_8 octa-functional cage (T_8R_8) and then closing the resulting silanotriol $T_7R_7(OH)_3$ to form the monofunctional POSS (T_8R_7R') cage. While the closing step is typically uncomplicated, reopening the cage lacks selectivity, resulting in a mixture of different silanotriol isomers. Our findings proved that this mixture poses challenges in synthesizing bifunctional $T_8R_6R'_2$ cages. The performed study highlights the hindrance caused by the crystallization of a stable dimer in further cage corner-capping reactions. Computational methods were used to analyze this issue and evaluate mono-cages' reactivity in both open and closed states. It was observed that dimers exhibit greater stability and are prevalent in the crystalline form, while monomers dominate the solution. The theoretical investigations provided insights into the factors influencing the transition of silanotriol structures from monomers to dimers. Moreover, cages with different substituents and side reactive arms showed varying reactivity in corner-capping reactions.

In silsesquioxane cage chemistry, finding solutions to control selective reactions involving the closing and opening of monofunctional cages remains challenging and intriguing. The study lays the groundwork for designing effective synthesis strategies and understanding the reactivity of POSS cages with different sidearms. At the moment, this will require further research, optimization of synthesis conditions, supported by quantum calculations.

Conflicts of interest

There are no conflicts to declare.

Acknowledgements

This work was financially supported by the National Science Centre, Poland (Grant No. 2020/39/B/ST4/00910) and the Wrocław Centre for Networking and Supercomputing (**https://www.wcss.wroc.pl**) by providing computational time and facilities.

References

1 C. Hartmann-Thompson, *Applications of Polyhedral Oligomeric Silsesquioxanes*, Springer, New York, 2011.

2 A. Władyczyn, A. Gągor, K. Ślepokura and Ł. John, Hydroxyalkyl-substituted double-decker silsesquioxanes: effective separation of cis and trans isomers, *Inorg. Chem. Front.*, 2022, **9**, 3999–4008.

3 D. B. Cordes, P. D. Lickiss and F. Rataboul, Recent Developments in the Chemistry of Cubic Polyhedral Oligosilsesquioxanes, *Chem. Rev.*, 2010, **110**, 2081–2173.

4 D. A. Tomalia, J. B. Christensen and U. Boas, *Dendrimers, Dendrons, and Dendritic Polymers: Discovery, Application, and the Future*, Cambridge University Press, Cambridge, UK, 2012.

5 G. M. Whitesides and B. Grzybowski, Self-Assembly at all Scales, *Science*, 2002, **295**, 2418–2421.

6 M. Laird, N. Herrmann, N. Ramsahye, C. Totée, C. Carcel, M. Unno, J. R. Bartlett and M. Wong Chi Man, Large Polyhedral Oligomeric Silsesquioxane Cages: The Isolation of Functionalized POSS with Unprecedented $Si_{18}O_{27}$ Core, *Angew. Chem., Int. Ed.*, 2021, **60**, 3022–3027.

7 B. Dudziec and B. Marciniec, Double-decker Silsesquioxanes: Current Chemistry and Applications, *Curr. Org. Chem.*, 2017, **21**, 2794–2813.

8 A. Mrzygłód, M. Kubicki and B. Dudziec, Vinyl- and chloromethyl-substituted mono-T_8 and double-decker silsesquioxanes as specific cores to low generation dendritic systems, *Dalton Trans.*, 2022, **51**, 1144–1149.

9 K. Naka and Y. Irie, Synthesis of single component element-block materials based on siloxane-based cage frameworks, *Polym. Int.*, 2017, **66**, 187–194.

10 M. Wang, H. Chi, K. S. Joshy and F. Wang, Progress in the Synthesis of Bifunctionalized Polyhedral Oligomeric Silsesquioxane, *Polymers*, 2019, **11**, 2098.

11 J. Kaźmierczak, D. Lewandowski and G. Hreczycho, B$(C_6F_5)_3$-Catalyzed Dehydrocoupling of POSS Silanols with Hydrosilanes: A Metal-Free Strategy for Effecting Functionalization of Silsesquioxanes, *Inorg. Chem.*, 2020, **59**, 9206–9214.

12 K. Kuciński and G. Hreczycho, A Highly Effective Route to Si-O-Si Moieties through O-Silylation of silanols and Polyhedral Oligomeric Silsesquioxane Silanols with Disilazanes, *ChemSusChem*, 2019, **12**, 1043–1048.

13 A. Mrzygłód, R. Januszewski, J. Duszczak, M. Dutkiewicz, M. Kubicki and B. Dudziec, Tricky but repeatable synthetic approach to branched, multifunctional silsesquioxane denrimer derivatives, *Inorg. Chem. Front.*, 2023, **10**, 4587–4596.

14 X.-M. Wang, Q.-Y. Guo, S.-Y. Han, J.-Y. Wang, D. Han, Q. Fu and W.-B. Zhang, Stochastic/Controlled Symmetry Breaking of the T_8-POSS Cages toward Multifunctional Regioisomeric Nanobuilding Blocks, *Chem. – Eur. J.*, 2015, **21**, 15246–15255.

15 T. Maegawa, Y. Irie, H. Imoto, H. Fueno, K. Tanaka and K. Naka, para-Bisvinylhexaisobutyl-substituted T_8 caged monomer: synthesis and hydrosilylation polymerization, *Polym. Chem.*, 2015, **6**, 7500–7504.

16 B. J. Hendan and H. C. Marsmann, Semipräparative Trennung gemischt substituierter Octa-(organylsilsesquioxane) mittels Normal-Phase-HPLC und ihre ^{29}Si-NMR-spektroskopische Unters, *J. Organomet. Chem.*, 1994, **483**, 33–38.

17 M. Bołt, P. Żak, B. Dudziec, A. Schulmann and B. Marciniec, Formation of Bifunctional Octasilsesquioxanes via Silylative Coupling and Cross-Metathesis Reaction, *Materials*, 2020, **13**, 3966.

18 M. G. Voronkov and V. I. Lavrent'yev, Polyhedral oligosilsesquioxanes and their homo derivatives, in *Inorganic Ring Systems, Topics in Current Chemistry*, Springer, Berlin, Heidelberg, 1982, pp. 199–236.

19 T. N. Martynova and T. I. Chupakhina, Heterofunctional oligoorganylsilsesquioxanes, *J. Organomet. Chem.*, 1988, **345**, 10–18.

20 M. Z. Asuncion and R. M. Laine, Fluoride Rearrangement Reactions of Polyphenyl- and Polyvinylsilsesquioxanes as a Facile Route to Mixed Functional Phenyl, Vinyl T_{10} and T_{12} Silsesquioxanes, *J. Am. Chem. Soc.*, 2010, **132**, 3723–3736.

21 F. Carniato, E. Boccaleri and L. Marchese, A versatile route to bifunctionalized silsesquioxane (POSS): synthesis and characterisation of Ti-containing aminopropylisobutyl-POSS, *Dalton Trans.*, 2007, 36–39.

22 T. Maegawa, Y. Irie, H. Fueno, K. Tanaka and K. Naka, Synthesis and Polymerization of a para-Disubstituted T_8-caged Hexaisobutyl-POSS Monomer, *Chem. Lett.*, 2014, **43**, 1532–1534.

23 I. Blanco, L. Abate, F. A. Bottino and P. Bottino, Hepta isobutyl polyhedral oligomeric silsesquioxanes (hib-POSS), *J. Therm. Anal. Calorim.*, 2012, **108**, 807–815.

24 A. D. Becke, Density-Functional Thermochemistry., III. The Role of Exact Exchange, *J. Chem. Phys.*, 1993, **98**, 5648–5652.

25 C. Lee, W. Yang and R. G. Parr, Development of the Colle-Salvetti Correlation-Energy Formula into a Functional of the Electron-Density, *Phys. Rev. B: Condens. Matter Mater. Phys.*, 1988, **37**, 785–789.

26 S. Grimme, A. Hansen, J. G. Brandenburg and C. Bannwarth, Dispersion-Corrected Mean-Field Electronic Structure Methods, *Chem. Rev.*, 2016, **116**, 5105–5154.

27 R. Ditchfield, W. J. Hehre and J. A. Pople, Self-Consistent Molecular-Orbital Methods. IX. An Extended Gaussian-Type Basis for Molecular-Orbital Studies of Organic Molecules, *J. Chem. Phys.*, 1971, **54**, 724–728.

28 M. J. Frisch, G. W. Trucks, H. B. Schlegel, G. E. Scuseria, M. A. Robb, J. R. Cheeseman, G. Scalmani, V. Barone, G. A. Petersson, H. Nakatsuji, X. Li, M. Caricato, A. V. Marenich, J. Bloino, B. G. Janesko, R. Gomperts, B. Mennucci, H. P. Hratchian, J. V. Ortiz, A. F. Izmaylov, J. L. Sonnenberg, D. Williams-Young, F. Ding, F. Lipparini, F. Egidi, J. Goings, B. Peng, A. Petrone, T. Henderson, D. Ranasinghe, V. G. Zakrzewski, J. Gao, N. Rega, G. Zheng, W. Liang, M. Hada, M. Ehara, K. Toyota, R. Fukuda, J. Hasegawa, M. Ishida, T. Nakajima, Y. Honda, O. Kitao, H. Nakai, T. Vreven, K. Throssell, J. A. Montgomery Jr., J. E. Peralta, F. Ogliaro, M. J. Bearpark, J. J. Heyd,

E. N. Brothers, K. N. Kudin, V. N. Staroverov, T. A. Keith, R. Kobayashi, J. Normand, K. Raghavachari, A. P. Rendell, J. C. Burant, S. S. Iyengar, J. Tomasi, M. Cossi, J. M. Millam, M. Klene, C. Adamo, R. Cammi, J. W. Ochterski, R. L. Martin, K. Morokuma, O. Farkas, J. B. Foresman and D. J. Fox, Gaussian, Inc., Wallingford CT, 2016.

29 G. A. Zhurko, *Chemcraft - graphical software for visualization of quantum chemistry computations. Version 1.8*, **https://www.chemcraftprog.com**.

30 A. Gierer and K. Z. Wirtz, Molekulare Theorie der Mikroreibung, *Z. Naturforsch., A: Astrophys., Phys. Phys. Chem.*, 1953, **8**, 532–538.

31 H.-C. Chen and S.-H. Chen, Diffusion of Crown Ethers In Alcohols, *J. Phys. Chem.*, 1984, **88**, 5118–5121.

32 S. H. Chen and S. K.-H. Wei, Modification of the Stokes-Einstein Equation with a Semiempirical Microfriction Factor for Correlation of Tracer Diffusivities in Organic Solvents, *Ind. Eng. Chem. Res.*, 2011, **50**, 12304–12310.

33 T. Lu and F. Chen, Quantitative analysis of molecular surface based on improved Marching Tetrahedra algorithm, *J. Mol. Graphics Modell.*, 2012, **38**, 314–323.

34 T. Lu and F. Chen, Multiwfn: a multifunctional wavefunction analyzer, *J. Comput. Chem.*, 2012, **33**, 580–592.

35 W. Humphrey, A. Dalke and K. Schulten, VMD: Visual molecular dynamics, *J. Mol. Graphics Modell.*, 1966, **14**, 33–38.

36 F. J. Feher, R. Terroba and J. W. Ziller, A new route to incompletely-condensed silsesquioxanes: base-mediated cleavage of polyhedral oligosilsesquioxanes, *Chem. Commun.*, 1999, 2309–2310.

37 H. Liu, S. Kondo, R. Tanaka, H. Oku and M. Unno, A spectroscopic investigation of incompletely condensed polyhedral oligomeric silsesquioxanes (POSS-mono-ol, POSS-diol and POSS-triol): Hydrogen-bonded interaction and host-guest complex, *J. Organomet. Chem.*, 2008, **693**, 1301–1308.

38 M. D. Jones, C. G. Keir, A. L. Johnson and M. F. Mahon, Crystallographic characterization of novel Zn(II) silsesquioxane complexes and their application as initiators for the production of polylactide, *Polyhedron*, 2010, **29**, 312–316.

39 F. J. Feher, D. A. Newman and J. F. Walzer, Silsesquioxanes as Models for Silica Surfaces, *J. Am. Chem. Soc.*, 1989, **111**, 1741–1748.

40 S. Spirk, M. Nieger, F. Belaj and R. Pietschnig, Formation and hydrogen bonding of a novel POSS-trisilanol, *Dalton Trans.*, 2009, 163–167.

41 E. Nizioł, D. Jędrzkiewicz, A. Wiencierz, W. Paś, D. Trybuła, W. Zierkiewicz, A. Marszałek-Harych and J. Ejfler, Sodium complexes as precise tools for cutting polymer chains. Exploration of PLA degradation by unique cooperation of sodium centers, *Inorg. Chem. Front.*, 2023, **10**, 1076–1090.